



ELSEVIER

Contents lists available at ScienceDirect

Biosensors and Bioelectronics

journal homepage: www.elsevier.com/locate/bios

Short communication

A water-soluble carboxylic-functionalized chemosensor for detecting Al^{3+} in aqueous media and living cells: Experimental and theoretical studies



Jae Jun Lee^a, Gyeong Jin Park^a, Yong Sung Kim^a, Sun Young Lee^a, Hyun Ji Lee^b,
Insung Noh^b, Cheal Kim^{a,*}

^a Department of Fine Chemistry and Department of Interdisciplinary Bio IT Materials, Seoul National University of Science and Technology, Seoul 139-743, Korea

^b Department of Chemical and Biomolecular Engineering, and Convergence Program of Biomedical Engineering and Biomaterials, Seoul National University of Science & Technology, Seoul 139-743, Korea

ARTICLE INFO

Article history:

Received 19 November 2014

Received in revised form

29 January 2015

Accepted 25 February 2015

Available online 26 February 2015

Keywords:

Water-soluble

Aluminum

Carboxylic-functionalized

Bio-imaging

Theoretical calculations

ABSTRACT

A new water-soluble carboxylic-functionalized chemosensor **1** was designed and synthesized. **1** exhibited the selective fluorescence enhancement toward aluminum ions with a 1:1 complexation stoichiometry in aqueous solution. The detection limit (24 nM) of **1** for Al^{3+} is about two order lower than the WHO guideline (7.41 μM) for the drinking water. **1** was successfully applied to living cells and real samples for detecting Al^{3+} . Moreover, the sensing mechanism originated from the inhibited excited-state intramolecular proton transfer (ESIPT) process and the chelation-enhanced fluorescence (CHEF) effect, as supported by theoretical calculations.

© 2015 Elsevier B.V. All rights reserved.

1. Introduction

Aluminum is widely used in modern life, such as in pharmaceutical gastric antacids, food additives, utensils, and cosmetics. Owing to these wide usages, human beings are exposed to excessive Al^{3+} through direct intake or through the epidermis. The excess Al^{3+} are then deposited in various tissues, including bone, muscle, heart, spleen, liver, and brain, making the organs functionally disordered (Verstraeten et al., 2008). Particularly, Al^{3+} affects the central nervous system and is a potential factor in neurodegenerative diseases, such as Alzheimer's and Parkinson's diseases (Yokel, 2002). Recent studies show that aluminum salts used for antiperspirants in underarm cosmetics triggers carcinogenesis at the breasts by interfering with the function of estrogen receptors (Darbre, 2005). Besides these human toxicities, Al^{3+} also has adverse impacts on plant growth (Rout et al., 2001). Therefore, it becomes important to monitor trace amounts (e.g., nanomolar concentration) of Al^{3+} in aqueous sample.

Recently, many analytical methods, such as electrochemical methods, atomic absorption spectroscopy and inductively coupled

plasma atomic emission spectroscopy have been applied to detect metal ions including Al^{3+} (Gulaboski et al., 2002). However, these analytical methods need lengthy processing methods and sophisticated equipment. By contrast, fluorescence sensing methods can detect interesting analytes with fast response, convenient procedures, and high sensitivity. For this reason, scientists have devoted huge efforts to design fluorescence chemosensors for monitoring Al^{3+} (Das et al., 2012). Some of the reported Al^{3+} sensors showed their own unique advantages (Shellaiah et al., 2013; Chun-Yan et al., 2013; Shymarprosad et al., 2013; Shyamarprosad et al., 2013), but they suffer partly from interference caused by other metal ions such as Ga^{3+} and Zn^{2+} (Shyamarprosad et al., 2013), poor water solubility, and tedious synthetic methods of preparation (Chun-Yan et al., 2013; Shymarprosad et al., 2013).

A Schiff base, with π electrons in C=N group offers a good possibility for chelation with metal ions and can enhance the fluorescence through CHEF mechanism (Kim et al., 2012). In this regard, a julolidine moiety is a well-known chromophore and chemosensors with the julolidine moiety are usually water-soluble (Choi et al., 2014). Moreover, we expected that the presence of carboxylate group (a hard base) in a chemosensor might not only increase its water solubility, but also would make the molecule more selective toward a hard acid, such as Al^{3+} . Therefore, we

* Corresponding author. Fax: +82 2 973 9149

E-mail address: chealkim@seoultech.ac.kr (C. Kim).

planned to develop a simple Schiff base chemosensor with both a julolidine group and a carboxylate group. In the current work, a new Schiff base chemosensor **1** ((E)-2-(((8-hydroxy-2,3,6,7-tetrahydro-1H,5H-pyrido[3,2,1-ij]quinolin-9-yl)methylene)amino)benzoic acid) was synthesized, which contained both the julolidine and the carboxylic acid groups. The molecule **1** showed a good water solubility and the sensing abilities of **1** were tested toward various metal ions. Indeed, the receptor **1** exhibited an exclusive sensing property towards Al^{3+} even at nanomolar concentration in various solvent systems via fluorescence. Additionally, the theoretical calculations supported the experimental data and the sensing mechanism.

2. Material and methods

Reagent, instruments, experimental methods and theoretical calculation methods are given in Supplementary information (SI).

3. Results and discussion

3.1. Synthesis

The receptor **1** was obtained by coupling anthranilic acid with 8-hydroxyjulolidine-9-carboxaldehyde with an 87% yield in ethanol (Scheme S1) and analyzed by ^1H NMR, ^{13}C NMR, ESI-mass spectrometry and elemental analysis.

3.2. Fluorescence and absorption spectroscopic studies of **1** toward Al^{3+} ion

To examine the fluorescent properties of **1**, the emission was measured with various metal ions (Na^+ , K^+ , Mg^{2+} , Ca^{2+} , Al^{3+} , Ga^{3+} , In^{3+} , Cr^{3+} , Mn^{2+} , Fe^{2+} , Fe^{3+} , Co^{2+} , Ni^{2+} , Cu^{2+} , Zn^{2+} , Cd^{2+} , and Pb^{2+}) in a variety of solvent systems such as methanol (MeOH), dimethylsulfoxide (DMSO), dimethylformamide (DMF), and bis-tris buffer solution (10 mM, pH 7.0) containing 50% DMSO. Importantly, only Al^{3+} showed fluorescence enhancement as shown in Fig. 1 and S1, while most chemosensors with only a julolidine moiety did it not only for Al^{3+} but also for Ga^{3+} and In^{3+} .

These results demonstrate that the presence of carboxylate group as a hard base in a chemosensor might be more selective towards the hard acid, Al^{3+} .

For practical purposes, the sensing properties of **1** toward Al^{3+} were further examined in bis-tris buffer solution (10 mM, pH 7.0) containing 50% DMSO. Receptor **1** exhibited fluorescence with a low quantum yield ($\Phi = 3.81 \times 10^{-4}$), which was much lower than that ($\Phi = 0.143$) in the presence of Al^{3+} with excitation at 478 nm (Fig. 1). The substantial fluorescence enhancement of **1** might be explained by the restricted ESIP (Wang et al., 2014) involving the phenolic protons (Scheme 1). Also, the selective fluorescence enhancement by Al^{3+} might be due to the effective coordination of Al^{3+} to **1**, imparting the CHEF effect (Supriti et al., 2012; Kim et al., 2012).

The fluorescence titration experiment of **1** with Al^{3+} showed that the emission intensity of **1** at 478 nm steadily increased until the amount of Al^{3+} reached 42 equiv (Fig. S2). UV-vis titration of **1** was also conducted with Al^{3+} (Fig. S3). Upon the addition of Al^{3+} to a solution of **1**, the absorption band at 435 nm decreased, while a new band at 380 nm increased ($\epsilon = 1.2 \times 10^4 \text{ L mol}^{-1} \text{ cm}^{-1}$). Two isosbestic points were observed at 393 and 498 nm, suggesting that only one product was produced from the binding of **1** with Al^{3+} .

The Job plot referred to a 1:1 stoichiometric complex between **1** and Al^{3+} (Fig. S4), and this was further confirmed by ESI-mass spectrometry analysis (Fig. S5). The positive-ion mass spectrum showed a large peak at 516.60 m/z, which was assignable to 1- Al^{3+} complex + 3 solvents [calcd, m/z: 516.22]. Based on the Job plot, ESI-mass spectrometry analysis, and the crystal structures of similar type of Al complexes reported in the literatures (Myers and Berben 2011), a penta-coordinated structure for the 1- Al^{3+} complex with two solvent molecules or nitrates was proposed (Scheme 1).

The association constant (K) of the 1- Al^{3+} complex was determined to be $1.0 \times 10^4 \text{ M}^{-1}$ by using non-linear fitting analysis (Fig. S6), which is within the range of those ($10^3 \sim 10^9$) reported for Al^{3+} binding chemosensor. The detection limit estimated, based on the $3\sigma/\text{slope}$, was 24 nM, (Fig. S7), which was about two order lower than the WHO guideline (741 μM) for Al^{3+} in the drinking water (Alstad et al., 2005; Han et al., 2012), and comparable to those of the Al^{3+} chemosensors reported to show the lowest

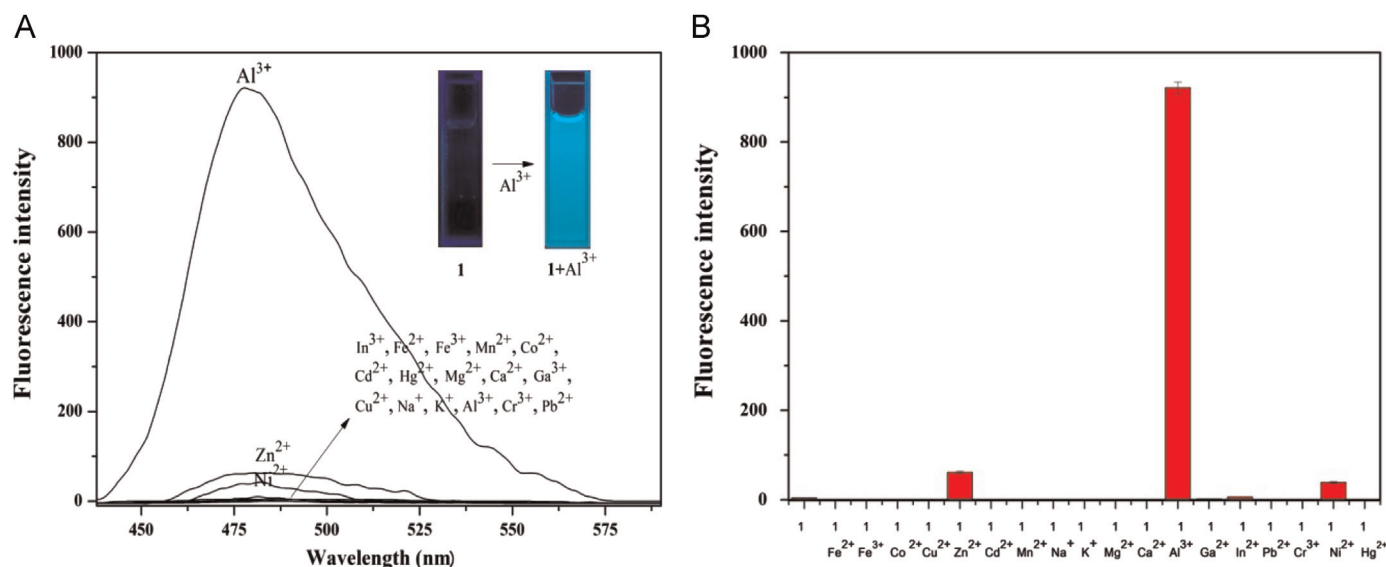
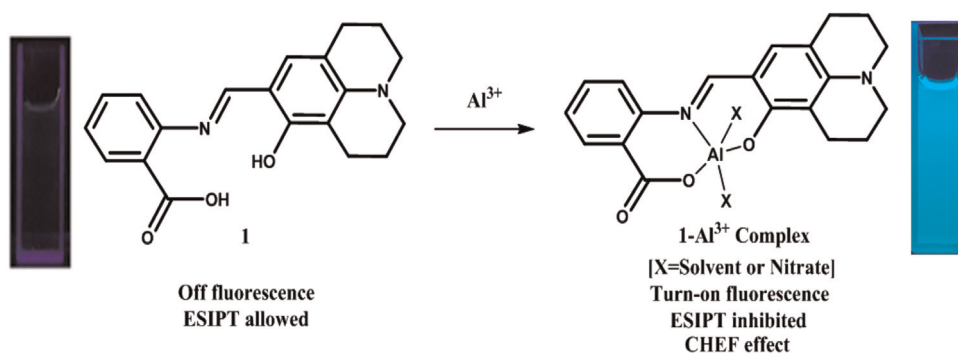


Fig. 1. (A) Fluorescence spectra of **1** ($5 \mu\text{M}$) upon addition of various metal ions (42 equiv) of Na^+ , K^+ , Mg^{2+} , Ca^{2+} , Al^{3+} , Ga^{3+} , In^{3+} , Cr^{3+} , Mn^{2+} , Fe^{2+} , Fe^{3+} , Co^{2+} , Ni^{2+} , Cu^{2+} , Zn^{2+} , Cd^{2+} , and Pb^{2+} in DMSO-buffer solution (10 mM bis-tris, pH 7.0, v/v = 1:1, $\lambda_{\text{ex}} = 420 \text{ nm}$). Inset: Picture of the fluorescence corresponded with **1** and 1- Al^{3+} (Excitation: 365 nm) (B) Bar graph representing the change of the relative emission intensity of **1** at 365 nm upon treatment with various metal ions.



detection limits (Bodenant et al., 1998). For practical applications, we carried out fluorescence titration in three real samples, tap, distilled, and pond waters. The detection limits for the real samples were determined to be 37 nM (tap water), 47 nM (distilled water) and 60 nM (pond water), based on the $3\sigma/\text{slope}$ (Fig. S8 and Table S1). These results suggest that the receptor **1** could be used to monitor trace amounts of Al^{3+} in environmental solutions.

To further check the practical applicability of receptor **1** as Al^{3+} selective sensor, fluorescence interference experiment was carried out in presence of various competing metal cations (Fig. S9). Other background metal ions had small or no obvious interference with the detection of Al^{3+} ion, except for three metal ions, viz. Cr^{3+} , Fe^{2+} and Fe^{3+} , which are strong quenchers of fluorescence (Bodenant et al., 1998). Nevertheless, these results suggest that **1** could be a good sensor for Al^{3+} and, in particular, can differentiate Al^{3+} from Ga^{3+} and In^{3+} , where all three have many similar properties.

The effect of pH on the fluorescence response of receptor **1** to Al^{3+} ion was also investigated in a series of buffers with pH values ranging from 2 to 11 (Fig. S10). An intense and stable fluorescence of the **1**- Al^{3+} complex was retained between pH 3.0 and 8.0. These results indicate that Al^{3+} could be clearly detected by the fluorescence measurements using **1** over the wide pH range of 3.7–8.0, which includes the biologically relevant range of pH 6.0–7.6.

3.3. In vitro cellular studies of **1** toward Al^{3+} ion

Based on the pH dependence, subsequent experiments were conducted to test whether **1** could be used to visualize intracellular Al^{3+} by fluorescence or not. Adult human dermal fibroblasts were first incubated with various concentrations of Al^{3+} (0, 20, 50, 100 and 200 μM) for 4 h and then exposed to **1** (50 μM)

for 1 h before imaging. The fibroblasts that were cultured with both Al^{3+} and **1** exhibited fluorescence (Fig. 2), while those cells cultured without Al^{3+} or without **1** did not exhibit any fluorescence. The intensity and region of the fluorescence within the cell with **1** increased as the Al^{3+} concentration increased from 20 to 200 μM . The mean fluorescence intensity of the microscopy images in Fig. 2 was evaluated by Icy software (Fig. S11). The detection limit was found to be 1.9 μM , which is still a below the WHO guideline for Al^{3+} in the drinking water. In order to further confirm that the increase of the fluorescence depended on the Al^{3+} changes (Nandre et al., 2014), the Al^{3+} -supplemented cells (Fig. S12B and E) were treated with 100 μM of metal chelator (desferoxamine: DFO) to remove the intracellular levels of Al^{3+} . The intracellular fluorescence disappeared with the DFO chelation (Fig. S12C and F), demonstrating that the observed intracellular fluorescence enhancements (Fig. S12B and E) were due to the changing levels in the Al^{3+} -supplemented cells. Moreover, the biocompatibility of **1** was also examined with the living cells (Fig. S13). All the fibroblasts were still alive until 12 h, while some cells were dead after 24 h. These results confirm that **1** can be a suitable and biocompatible sensor to detect Al^{3+} in living cells.

3.4. ^1H NMR titration of **1** with Al^{3+}

In order to further investigate the binding mode between **1** and Al^{3+} , ^1H NMR titration was conducted in $\text{DMSO}-d_6$ (Fig. S14). While the non-aromatic protons of the julolidine moiety in **1** changed little, the aromatic and imine protons (H_1 , H_2 , H_3 , H_4 , H_5 , and H_6) were shifted to downfield. These results indicate that Al^{3+} might be coordinated to two oxygens of carboxylate and phenol groups and nitrogen of imine moiety, as proposed in Scheme 1. On further addition of Al^{3+} (> 1 equiv) into **1** solution, no shift in the

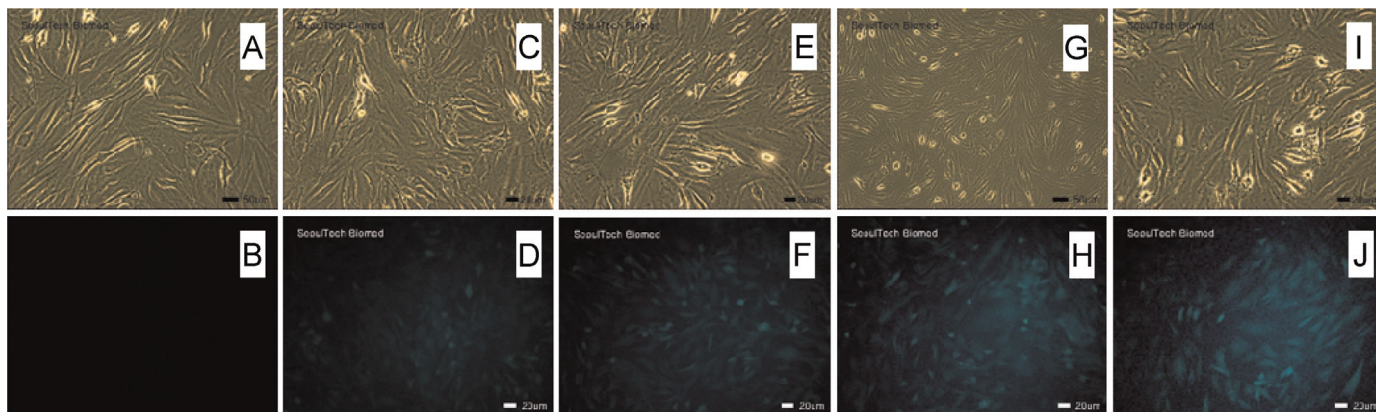


Fig. 2. Fluorescence images of fibroblasts cultured with Al^{3+} and **1**. Cells were exposed to 0 (A and B), 20 (C and D), 50 (E and F), 100 (G and H) and 200 (I and J) μM $\text{Al}(\text{NO}_3)_3$ for four hours and then later with **1** (50 μM) for 1 hour. The top images (A, C, E, G, and I) were observed using a light microscope and the bottom images were taken using a fluorescence microscope. The scale bar is 20 μm .

position of proton signals was observed, which supports a 1:1 complexation of **1** with Al^{3+} .

3.5. Theoretical calculations

To obtain a deeper insight into the interaction of **1** and Al^{3+} , theoretical calculations were also done in parallel to the experimental studies. Energy-minimized structures (S_0) for **1** and **1**- Al^{3+} complex were optimized by applying density functional theory (DFT/B3LYP/6-311G**) (Becke, 1993) in water solution (CPCM) (Cossi et al., 2003) with GAUSSIAN 03 program (Frisch et al., 2004) (Fig. S15). Time-dependent density functional theory (TD-DFT) method was also performed at the energy-minimized structures of **1** and **1**- Al^{3+} complex (Fig. S15). In case of **1** (S_0), the main transition of the first excited state ($S_0 \rightarrow S_1$) was determined for HOMO to LUMO transitions (412 nm, $\pi \rightarrow \pi^*$) (Table S2 (a) and Fig. S16). In case of **1**- Al^{3+} complex, the main transition of the first excited state ($S_0 \rightarrow S_1$) was also determined for HOMO to LUMO transitions (414 nm, $\pi \rightarrow \pi^*$) (see Table S2 (b) and Fig. S17). These results are well consistent with the experimental absorption wavelengths (430 nm for **1** and 435 nm for **1**- Al^{3+} complex) within 20–30 nm deviations.

To figure out whether ES IPT for **1** would play an important role in the weak fluorescence of **1**, the potential energy surface (PES) scan was conducted between two tautomers, keto (c) and enol (a) (Fig. S18). In the ground state, the proton transfer from a (enol) to c (keto) and vice versa could occur with an energy barrier of 4.68 kcal/mol and 3.61 kcal/mol, respectively. This indicated that the enol form of **1** was more stable than its keto form by 1.08 kcal/mol energy. These results were consistent with the ^1H NMR spectrum of **1**, which showed chemical shift of the enol form. In the first excited state, the energy of keto form (c') was lower than that of enol form (a'). The potential energy curve for the excited state exhibited the energy barrier of 0.02 kcal/mol (from a' to b'), which was sufficiently small to allow proton transfer (H_{27}) from O_{26} to N_{30} in **1** (Chen et al., 2014). Thus, upon coordination with Al^{3+} , the ES IPT process for **1** was inhibited, resulting in the large fluorescence enhancement.

As the CHEF effect was also proposed as another sensing mechanism of **1** toward Al^{3+} , the optimized geometries of **1** and **1**- Al^{3+} complex were compared in the S_0 state. The geometry of the **1**- Al^{3+} complex showed a more planar and rigid structure than that of **1** (Fig. S19). As the rigid complex might inhibit the non-radiative processes, the CHEF effect also plays an important role in the fluorescence enhancement. Based on the Franck–Condon principle (Condon, 1928), the first excited state (S_1) of **1**- Al^{3+} complex was optimized by TD-DFT method. The optimized geometry of the S_1 state (**1**- Al^{3+}) showed a more coplanar structure than that of the S_0 state (**1**- Al^{3+}) (Fig. S19). This conformation relaxation led to a non-radiative process, and affected the energy level of the molecular orbitals. As shown in Fig. S20, the HOMO–LUMO energy gap decreased in the S_1 state geometry of **1**- Al^{3+} (blue arrow), compared to that in the S_0 state geometry of **1**- Al^{3+} (red arrow). These results suggest that the decrease in the HOMO–LUMO energy gap and the geometry relaxation were the main contributing factor for the large stoke shift. The theoretical emission wavelength of **1**- Al^{3+} complex was calculated to be 478 nm, which was in good agreement with the experimental value (477 nm) (Table S2 (c)). Therefore, a rigid structure and theoretical emission of **1**- Al^{3+} complex could support the sensing mechanism of Al^{3+} by the CHEF effect.

4. Conclusion

In this study, a carboxylic-functionalized chemosensor **1** was developed for detection of Al^{3+} ion in aqueous solution. **1** showed highly selective fluorometric response to Al^{3+} with the detection limit at the nanomolar level (24 nM). **1** could be successfully applied to living cells and real samples for detecting Al^{3+} . Moreover, the theoretical calculations supported the sensing mechanisms of Al^{3+} by **1**, which were proposed with the inhibited ES IPT and CHEF effects. Future study will focus on developing a chemosensor with the detection limit of picomolar level and its potential applications in biological chemistry.

Acknowledgements

Basic Science Research Programs through the National Research Foundation of Korea (NRF) (NRF-2014R1A2A1A11051794, 2012001725 and 2012008875) are gratefully acknowledged. We thank Nano-Inorganic Laboratory, Department of Nano & Bio Chemistry, Kookmin University to access the Gaussian 03 program packages.

Appendix A. Supplementary material

Supplementary data associated with this article can be found in the online version at <http://dx.doi.org/10.1016/j.bios.2015.02.038>.

References

- Alstad, N.E.W., Kjelsberg, B.M., Vøllestad, L.A., Lydersen, E., Poléo, A.B.S., 2005. *Environ. Pollut.* 133, 333–342.
- Becke, A.D., 1993. *J. Chem. Phys.* 98, 5648–5652.
- Bodenant, B., Fages, F., Delville, M., 1998. *J. Am. Chem. Soc.* 120, 7511–7519.
- Chen, J.S., Zhou, P.W., Zhao, L., Chu, T.S., 2014. *RSC Adv.* 4, 254–259.
- Choi, Y.W., Park, G.Y., Na, Y.U., Jo, H.Y., Lee, S.A., You, G.R., Kim, C., 2014. *Sens. Actuators B* 194, 343–352.
- Chun-Yan, L., Yu, Z., Young-Fei, L., Chun-Xiang, Zou, Xue-Fei, Kong, 2013. *Sens. Actuators B* 186, 360–366.
- Condon, E.U., 1928. *Phys. Rev.* 32, 858–872.
- Cossi, M., Scalmani, G., Rega, N., Barone, V., 2003. *J. Comp. Chem.* 24, 669–681.
- Darbre, P.D., 2005. *J. Inorg. Biochem.* 99, 1912–1919.
- Das, S., Lohar, S., Banerjee, A., Sahana, A., Das, D., 2012. *Anal. Methods* 4, 3620–3624.
- Frisch, M.J., et al., 2004. *Gaussian 03, Revision D.01*, G. Gaussian, Inc., Wallingford CT, USA.
- Gulaboski, R., Mirčeski, V., Scholz, F., 2002. *Electrochem. Commun.* 4, 277–283.
- Han, T., Feng, X., Tong, B., Shi, J., Chen, L., Zhi, J., Dong, Y., 2012. *Chem. Commun.* 48, 416–418.
- Kim, S., Noh, J.Y., Kim, K.Y., Kim, J.H., Kang, H.K., Nam, S.W., Kim, S.H., Park, S.S., Kim, C., Kim, J., 2012. *Inorg. Chem.* 51, 3597–3602.
- Myers, T.W., Berben, L.A., 2011. *J. Am. Chem. Soc.* 133, 11865–11867.
- Nandre, J., Patil, S., Patil, V., Yu, F., Chen, L., Sahoo, S., Prior, T., Redshaw, C., Mahulikar, P., Patil, U., 2014. *Biosens. Bioelectron.* 61, 612–617.
- Rout, G.R., Roy, S., Das, P., 2001. *Agronomie* 21, 3–21.
- Shyamaprosad, G., Sima, P., Abhishek, M., 2013. *RSC Adv.* 3, 25079–25085.
- Shymarprosad, G., Krishnendu, A., Sangita, D., Avijit, K.D., Deblina, S., Sukanya, P., Tapan, K.M., Subhrakanti, M., 2013. *Chem. Commun.* 49, 10739–10741.
- Shellaiah, M., Wu, Y., Lin, H., 2013. *Analyst* 138, 2931–2942.
- Supriti, S., Titas, M., Basab, C., Anuradha, M., Anupam, B., Jaromir, M., Pabitra, C., 2012. *Analyst* 137, 3975–3981.
- Verstraeten, S.V., Aimo, L., Oteiza, L.L., 2008. *Arch. Toxicol.* 82, 789–802.
- Wang, J., Chu, Q., Liu, X., 2014. *J. Phys. Chem. B* 117, 4127–4133.
- Yokel, R.A., 2002. *Coord. Chem. Rev.* 228, 97–113.